Miniaturized weak affinity chromatography for ligand identification of nanodiscs-embedded G-protein coupled receptors

Lucile Lecas, Lucie Hartmann, Lydia Caro, Sarah Mohamed-Bouteben, Claire Raingeval, Isabelle Krimm, Renaud Wagner, Vincent Dugas, Claire Demesmay

Ultra-miniaturized weak affinity chromatography for ligand identification of nanodiscs-solubilized G-protein coupled receptors

Lucile Lecas[#], Lucie Hartman[&], Lydia Caro[&], Sarah Mohamed-Bouteben[&], Claire Raingeval[#], Isabelle Krimm[#], Renaud Wagner[&], Vincent Dugas[#], Claire Demesmay[#]*

[#] Université de Lyon, CNRS, Université Claude Bernard Lyon 1, Institut des Sciences Analytiques, UMR 5280, 5 rue de la Doua, F-69100 VILLEURBANNE, France

[&] Plateforme IMPReSs, CNRS UMR7242, Biotechnologie et Signalisation Cellulaire, Ecole Supérieure de Biotechnologie de Strasbourg, Illkirch, France

ABSTRACT: Biophysical techniques that enable the screening and identification of weak affinity fragments against a target protein are at the heart of Fragment Based Drug Design approaches. In the case of membrane proteins, the crucial criteria for fragment screening are low protein consumption, unbiased conformational states and rapidity because of the difficulties in obtaining sufficient amounts of stable and functionally folded proteins. Here we show for the first time that lipid-nanodisc systems (membrane-mimicking environment) and ultra-miniaturized affinity chromatography can be combined to identify specific small molecule ligands that bind to an integral membrane protein. The approach is exemplified using the $AA_{2A}R$ GPCR. Home-made affinity nano-columns modified with nanodiscs-embedded $AA_{2A}R$ (only about 1 µg of protein per column) are fully characterized by frontal chromatographic experiments. This method allows (i) to distinguish specific and unspecific ligand/receptor interactions, (ii) to assess dissociation constants, (iii) to identify the binding pocket of uncharacterized ligands using a reference compound with competition experiments. Weak affinity ligands with K_d in the low to high micromolar range be detected. At last, the applicability of this method is demonstrated with 6 fragments recently identified as ligands or non-ligands of $AA_{2A}R$.

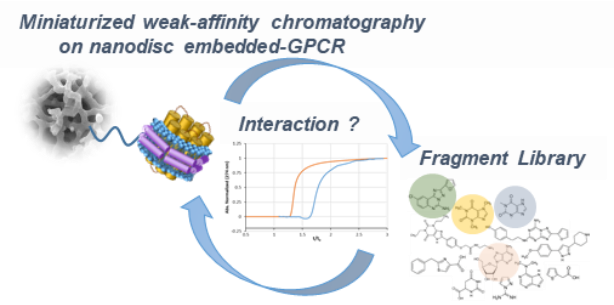

Integral membrane proteins represent 20-30% of the total proteins encoded in the human genome, including ion channels, transporters, receptors and enzymes. The G protein-coupled receptors (GPCRs) family is the most diversified family of membrane proteins and play a key role in nearly all physiological processes including vision, immune system, neurotransmission, cellular proliferation. As a consequence, GPCRs are involved in many diseases such as asthma, diabetes, Alzheimer disease and cancer, representing approximatively 30% of currently marketed therapeutic drug targets[1]. Still, 73% of the non-olfactory GPCRs remain untargeted[2], explaining why the pharmaceutical industry places intensive efforts on GPCR drug discovery programs and is seeking for innovative and robust drug screening methodologies.

Among these approaches, Structure-Based-Drug-Design (SBDD) applied to drugs targeting GPCRs appears highly promising but faces two main issues. Firstly, the overproduction of GPCRs leading to structure determination is challenging both in terms of quantities and stability. Because GPCRs are highly dynamics proteins that undergo a number of conformational changes upon ligand binding, this inherent conformational flexibility is actually a key issue for crystallographic structural studies. In the last decade, the implementation of GPCR-stabilization strategies, such as receptor mutagenesis, insertion of fusion proteins or use of antibody fragments[3], induced a major breakthrough in GPCR structural biology, which in turn opened the route for SBDD [4,5]. The second issue concerns the screening of novel ligands, and in particular weak affinity ligands such as fragments for the development of new drugs. Fragments are small molecules, with restricted physicochemical properties known as the rule of three. This rule suggests that fragments have limited molecular weight (< 300 g/mol), high solubility (logP > 3) and few hydrogen bond donors (<3) and acceptors (<3)[6]. Screening such small compounds is highly effective in terms of chemical space, and fragment libraries are usually composed of only one to several thousand molecules. The fragments hits that are identified typically display low to high µM affinities and are then elaborated into active compounds through a second step based on structural approaches. Identifying such small molecules, the first step of the Fragment-Based Drug Design (FBDD) process,

consists of screening fragments against a purified protein, using biophysical techniques, among which NMR, X-Ray crystallography and Plasmonic Surface Resonance (SPR) are the most extensively used[7] and other like weak affinity chromatography are currently under development[8–11] . Moreover while FBDD has been widely applied to soluble proteins[12], very limited reports illustrate some examples of fragment screening against membrane proteins and GPCRs[13–19].

Undoubtedly, there is a major need for the identification and elaboration of novel GPCR ligands and in particular for techniques that enable the screening and identification of weak affinity fragments. Ideally, such techniques should accommodate the GPCR-specific requirements discussed above *i.e.,* (i) minimize the sample size to fit the small amounts of purified GPCR that can be reasonably achieved, and (ii) be adapted to the dynamics and intrinsic conformational flexibility of the receptors in a membrane–like environment.

Among the variety of systems that have been developed over the years to investigate GPCRs in solution, lipid nanodiscs have particularly attracted attention for native GPCR interaction studies, most notably with techniques such as NMR and SPR[20–22]. Nanodiscs are self-assembled soluble discoidal phospholipids bilayers encircled by an amphipathic protein called Membrane Scaffold Protein (MSP)[23]. They have been proved to give the membrane proteins a native-like environment associated with a high homogeneity in size and a high solubility and stability in aqueous solution[24].

Here, we propose a strategy that combines the preparation of nanodiscs-embedded GPCRs and the ultra-miniaturization of weak affinity chromatography for the detection of GPCR-bound weak affinity fragments. In this approach, the nanodisc-embedded target is immobilized on the chromatographic support via the biotinylated nanodiscs. The primary innovations concern (i) the biomimetic assembly that allows the immobilization of a fully label-free and purified integral membrane protein, (ii) the immobilization strategy on a streptavidin generic monolithic column that allows an immediate (a few minutes) and in-situ UV-monitored grafting without any protein waste, (iii) the reduction of the protein consumption at the µg level for one reusable affinity column.

The technique is exemplified using the adenosine A_{2A} receptor ($AA_{2A}R$), a prototypical class A GPCR receptor. $AA_{2A}R$ has been extensively studied during the past few decades making it an ideal model with a large repertoire of ligands[25,26] and 3D X-ray structures available in the presence of antagonists, agonists and in complex with a G-protein[27]. Nevertheless, $AA_{2A}R$ remains a hot topic and the discovery of additional compounds could lead to numerous possibilities for therapeutics applications against inflammation, asthma, cardiovascular diseases, central nervous system diseases and cancer[28–31].

The home-made affinity nano-columns are fully characterized by frontal chromatographic experiments. It is demonstrated that specific and unspecific ligand/receptor interactions can be distinguished, that binding constants from low to high µM range can be determined and that the binding pocket of uncharacterized ligands can be assessed with competition experiments using a reference compound. At last, the applicability of this method for FBDD is demonstrated with 6 fragments recently identified as ligands or non-ligands of $AA_{2A}R$.

EXPERIMENTAL SECTION

Biochemistry Methods

Production and purification of $AA_{2A}R$

The wild-type human $AA_{2A}R$ receptor N-terminally fused to the flag and deca-histidine tags was recombinantly produced with the Pichia pastoris system as previously described[32]. $AA_{2A}R$ receptors were then prepared as follows. After cell lysis and whole membrane preparation[32], membranes were diluted to ca. 2 mg.mL^{-1} in cold solubilization buffer (50 mM HEPES pH 7.4, 500 mM NaCl, 0.5 % β-DDM (w/v), 0.05 % CHS (w/v), 25 mM imidazole, 1 µM DPCPX, 0.3 mM EDTA) containing an antiprotease cocktail (Roche). The suspension was incubated for 30 min at room temperature, followed by centrifugation at 100,000 x g for 30 minutes. Solubilized proteins were then loaded on a 1 mL HisTrap HP column (GE Healthcare) at 1 mL.min^{-1} flow rate. After extensive washing with a 50 mM HEPES pH 7.4, 500 mM NaCl, 0.05 % β-DDM (w/v), 0.005 % CHS (w/v), 25 mM imidazole, 1 µM DPCPX buffer, the bound receptor was eluted with a linear gradient of 25 to 500 mM imidazole. Fractions eluting at around 150 mM imidazole were pooled, concentrated down to 400-500 µL (Vivaspin 6, 30k MWCO), and loaded onto a Superdex 200 increase 10/300 GL column (GE Healthcare). Proteins were separated at 0.3 mL.min^{-1} with a 50 mM HEPES pH 7.4, 150 mM NaCl, 0.02 % β-DDM (w/v), 0.002 % CHS (w/v) 1 µM DPCPX buffer. Fractions containing the purified $AA_{2A}R$ receptor in detergent were pooled and directly used for reconstitution in lipid nanodiscs.

Membrane scaffold protein purification and biotinylation

The membrane scaffold protein MSP1E3D1(-) was produced and purified as previously described[33]. MSP1E3D1(-) was then incubated in presence of a biotinylation reagent (EZ-LinkTM NHS-PEG4-Biotin, Thermo Scientific) at a 1:5 MSP:biotin molar ratio in a 20 mM HEPES pH 7.4, 100 mM NaCl, 0.5 mM EDTA buffer. After a one-hour incubation at room temperature, the reaction was stopped by adding 5 mM Tris-HCl pH 7.4. The resulting biotinylated-MSP1E3D1(-) was isolated from the free reagent in a final desalting step (HiTrap desalting, GE Healthcare) in a 20 mM Tris-HCl pH 7.4, 100 mM NaCl, 0.5 mM EDTA storage buffer, flash-frozen in liquid nitrogen and stored at -80 °C until use. The actual biotinylation was further confirmed in a standard Western-blot revealed with extravidin-HRP.

Nanodisc assembly and purification

The biotinylated-MSP1E3D1(-) was mixed at a 1:70 molar ratio with purified lipids (POPC/POPG; 3/2 molar ratio) previously dissolved at a 24 mM concentration in a 50 mM HEPES pH 7.4, 150 mM NaCl, 48 mM Na-cholate buffer, and incubated for 15 minutes on ice. The purified receptor was then added to the MSP:lipid mixture at 1:10 receptor:MSP1E3(-) molar ratio and further incubated for 60 minutes on ice. Self-assembly was initiated by detergent removal using BioBeads SM-2 (Biorad) (0.25 g of Biobeads per mL of reconstitution mixture) and allowed to proceed overnight at 4 °C on a tube

rotator. The Biobeads were then removed by centrifugation and the recovered supernatant was directly loaded on a 1 mL HisTrap HP column (GE Healthcare) previously equilibrated in a 50 mM HEPES pH 7.4, 300 mM NaCl, 10 mM imidazole buffer. After extensive washing with the equilibration buffer, the $AA_{2A}R$-containing discs were eluted with the same buffer containing 500 mM imidazole. The eluted fractions were then pooled and loaded on a Superdex 200 10/300 GL column (GE Healthcare) previously equilibrated in a 50 mM HEPES pH7.4, 150 mM NaCl buffer. Elution was carried out at 0.3 $mL.min^{-1}$ and the fractions containing the pure $AA_{2A}R$-nanodiscs were finally aliquoted, flash-frozen in liquid nitrogen and stored at -80°C. The same procedure was followed for the preparation of empty nanodiscs, except that the MSP:lipids molar ratio was 1:130 instead of 1:70. In order to remove free lipids, empty nanodiscs were finally purified on a Superdex 200 10/300 GL column in the same conditions used for $AA_{2A}R$-nanodiscs.

Electron microscopy analysis

The nanodisc samples were diluted to approximately 0.2 $\mu g.mL^{-1}$ in purification buffer. Negative staining was performed using 2 % (w/v) uranyl acetate. Observation was carried out using a transmission electron microscope Philips CM 120 with a filament LaB6 (lanthanum hexaboride) at 120 kV. Images (Figure S1) were recorded at 45,000× magnification using a Gatan 794 CCD camera.

Competition ligand-binding assay

Competition ligand-binding assays were performed in triplicates using 5 nM of [3H]-ZM241385 as the tracer, and 10−10 to 10^{-3} M of competitor molecules. $AA_{2A}R$ in lipid discs (1 µg/mL) were incubated in 96-well plates in binding buffer (50 mM Tris-HCl pH 7.4, 10 mM $MgCl_2$, 1 mM EDTA). After 1 h incubation at room temperature, proteins were precipitated by supplementation with 0.1% gamma globulins and 25% PEG 6000 (Sigma-Aldrich) for 15 min. The reaction was stopped by rapid filtration through GF/B unifilters (Perkin Elmer) presaturated in 0.3% (v/v) PEI, followed by three successive washes with icecold buffer containing 50 mM Tris-HCl pH 7.4 and 8% (w/v) PEG 6000. Binding data were analyzed with the GraphPad Prism7 software (Figure S3). Inhibition constants (Ki) were calculated according to the Cheng-Prussof equation and were expressed as pKi.

Scintillation Proximity Assay (SPA)

The SPA assay was adapted from Hansen et al.[34]. Briefly, 100 ng of $AA_{2A}R$-nanodiscs, 100 ng of biotinylated-$AA_{2A}R$ purified in detergent, 60 ng of empty nanodiscs or 10 µg of membrane preparation samples were incubated in triplicates in 96-well plates (ProxiPlate-96, Perkin Elmer) in presence of 10 µL of streptavidin-coated yttrium silicate SPA beads (Perkin Elmer) and 25 nM of [3H]-ZM241385 in 100 µL final volume of binding buffer (50 mM Tris-HCl pH 7.4, 10 mM $MgCl_2$, 1 mM EDTA). Non-specific binding is determined in parallel in presence of 10 µM ZM241385. The sealed plate is then placed in a TopCount scintillation counter and measured every hour until 48 hours (Figure S4). Before the last measurement, proteins are denatured by adding 5 µL of 20% SDS to each well.

Chromatographic methods

Instruments

Nano-LC experiments (frontal weak affinity chromatography experiments) were carried out with a capillary electrophoresis Agilent HP3D CE system (Agilent Technologies, Waldbronn, Germany) equipped with external pressure nitrogen supply allowing to work up to 1.2 MPa. System control and data acquisition were carried out using the Chemstation software (Agilent). The experiments were conducted using the CE system in the so-called “short-end” injection mode. The system was exclusively operated in the pressurization mode by applying external pressure (no voltage applied). The inlet of the capillary column is simply immersed in the solution to be infused and the external pressure forces the liquid to flow inside the capillary column. The detection was achieved “on-column” (in an empty section of the 10-cm capillary located just after the monolith), with a diode array detector operated in a multi-wavelength mode. The effective length was 8.5 cm. Experiments were conducted under controlled room temperature (25°C).

Capillary monolith synthesis

Fused-silica capillaries with UV transparent coating (TSH, 75-µm i.d.) were purchased from Polymicro Technologies (Molex). Poly(GMA-co-EDMA) monoliths were synthesized as described in a previous work[35,36].

Streptavidin immobilization protocol

Streptavidin columns were prepared using the Schiff base method as previously described[37] (Streptavidin from streptomyces avidinii, affinity purified, ≥ 13 $U.mg^{-1}$ of protein, Sigma Aldrich)

RESULTS AND DISCUSSION

Preparation of nanodiscs-embedded $AA_{2A}R$

In this study, the wild-type human $AA_{2A}R$ receptor N-terminally fused to a Flag and a deca-histidine tags was produced with a yeast Pichia pastoris recombinant clone overexpressing the corresponding DNA construct[32,38]. After extraction from the yeast membranes and purification in presence of a DDM/CHS detergent mixture, $AA_{2A}R$ was further assembled in lipid nanodiscs similarly to previously described conditions[21]. For the purpose of the present affinity chromatography strategy, nanodisc particles have to be firmly immobilized on the chromatographic support. Therefore, the MSP employed here (i.e. MSP1E3D1) was in vitro biotinylated using a NHS-PEG4-Biotin reagent. While the resulting $AA_{2A}R$ nanodisc brings the receptor a stable membrane-mimicking environment compatible with an extensive use in dynamic conditions[34], it also allows a strong immobilization on streptavidin-coated supports via the biotin residues grafted on the MSP belt. Thanks to the presence of the PEG spacer arm that further maintains the assembly at distance from the support, the overall particle design thus ensures a full accessibility of the extramembrane domains of the receptor to the solvent and to any potential ligands it may contains.

The homogeneity of the nanodisc preparation was assessed by size exclusion chromatography and by negative staining electron microscopy (Figure S1), and the functionality of $AA_{2A}R$

in these nanodiscs was determined by ligand-binding assays performed in two different formats. In a first filtration-based competition binding assay, the pharmacology profiles of one agonist, adenosine, and three antagonist compounds, ZM241385, CGS15943 and xanthine amine congener (XAC) (Figure S2 for compounds structures) were evaluated (Figure S3). The pKi values obtained were relatively close to previously published data[39], indicating that the receptor was correctly folded in the nanodisc preparation. In a second format relying on the SPA technology (Scintillation Proximity Assay), radio-ligand binding was followed over time in order to evaluate the stability of $AA_{2A}R$ nanodiscs at room temperature. This assay revealed a consistent binding ability over time, with still about 50% of [3H]-ZM241385 bound after more than 40 hours of measurement (Figure S4). Overall, the quality and stability of the $AA_{2A}R$ nanodisc samples fulfilled the requirements of the planned WAC studies.

$AA_{2A}R$ affinity columns: preparation and evaluation with known ligands

One of the main objectives here was to drastically reduce the quantity of GPCR used for the characterization of GPCR-ligand interactions. Therefore, we used an in-house developed miniaturized affinity chromatographic column (75 µm internal diameter and 8.5 cm length i.e. less than 0.5 µL in volume). With their unique characteristics, these nano-columns have an internal diameter about 60 times smaller than commercially available affinity columns (4.6 mm i.d), and 7 times smaller than the smallest in-house microcolumns previously described in the literature for affinity studies (500 µm i.d)[40], which corresponds to a 3600-fold or a 50-fold reduction of the column volume, respectively. At this level of miniaturization, an in-situ synthesized poly(GMA-co-EDMA) monolith chromatographic support was preferred to conventional packed particulate ones. The epoxy surface groups of the monolith were then hydrolyzed into diols that were subsequently oxidized into aldehyde capable of reacting with streptavidin through Schiff base reaction[37]. The resulting streptavidin-coated columns were finally used to immobilize the biotinylated nanodiscs containing $AA_{2A}R$. The immobilization was performed dynamically, by simply flowing through the column a few microliters of a dilute solution of nanodisc-embedded $AA_{2A}R$ (µM range). The immobilization step was monitored using in-situ UV detection (Figure S5), in order to stop the sample flow once saturation is reached (no excess of protein consumed) and to quantify the total amount of nanodiscs captured. The typical immobilization step duration is quite short, viz about 10 minutes. For a set of 10 columns, around 14 pmol of protein were immobilized per column (14.2 ± 2.7 pmol, n= 10), which correspond to about 0.6 µg of $AA_{2A}R$-containing nanodiscs. These miniaturized and reusable affinity columns thus lead to a considerable reduction of protein consumption (less than 1 µg per column.

In order to assess the functionality of the column-immobilized $AA_{2A}R$ nanodiscs, frontal affinity chromatography (FAC) was used to study protein-ligand interactions. FAC is a powerful chromatographic tool for the measurement of protein-ligand binding constants and is particularly suitable for the analysis of weak interactions. With this approach, solutions of increasing ligand concentration were continuously infused into the affinity column until their breakthrough, due to saturation of the binding sites. The on-line UV signal monitoring (or ion current signal monitoring if a mass spectrometer is used as detector) gives a typical sigmoid-like profile, with front and plateau at the breakthrough time ($t_{plateau}$). Binding interaction between the ligand and the immobilized protein is characterized by an increase in breakthrough time with decreasing ligand concentration. If there is no specific interaction, the breakthrough time remains constant regardless of the ligand concentration[41]. Measuring the breakthrough times for several ligand concentrations permits to characterize the binding affinity, the amount of active proteins and to reveal potential non-specific interactions. Indeed, for each ligand concentration [L], the total amount of ligand captured in the column, q, can be experimentally determined using Equation (1):

$$q = (t_{plateau} - t_0) \times F \times [L] \qquad \text{(Eq.1)}$$

with F being the flow rate and t_0 the column dead time.

The total amount of ligand captured is the sum of what is specifically interacting within each protein binding sites and what is non-specifically interacting with the column surface and/or, in our case, with the nanodiscs particles, as shown in Equation (2):

$$q = \underbrace{\sum \left[\frac{B_{act,i} \times [L]}{K_{d,i} + [L]}\right]}_{\text{specific}} + \underbrace{K_{ns} \times [L]}_{\text{non-specific}} \qquad \text{(Eq.2)}$$

with $B_{act,i}$ being the amount of each protein active binding site i, $K_{d,i}$ the dissociation constants of the ligand interacting with each of them and K_{ns} the constant related to non-specific interactions.

If only non-specific interactions occur, Equation 2 becomes a linear equation and the amount of ligand captured varies proportionally to the applied ligand concentration. Otherwise, if non-specific interactions are negligible in comparison with specific ones, the type of interaction can be characterized by plotting a double reciprocal graph 1/q versus 1/[L]. Thus, a one-site interaction leads to a linear fit whereas a multi-site interaction leads to a non-linear fit. From there, the dissociation constants $K_{d,i}$ and the numbers of active sites $B_{act,i}$ can be determined by linear or non-linear regression[42].

In order to detect and quantify potential non-specific binding of ligands, the experiments carried out on $AA_{2A}R$-nanodiscs grafted columns were also simultaneously performed on empty-nanodiscs grafted columns. Regardless of the ligand concentration, the normalized breakthrough time $t_{plateau}/t_0$ is equal to 1 if no non-specific interactions occur, or constant and higher than 1 otherwise. This provides a simple and convenient negative control.

FAC experiments were performed with three well-characterized compounds, two antagonists, theophylline and caffeine, and one agonist, adenosine (see Figure S2 for compounds structures). The breakthrough curves obtained for theophylline are represented in Figure 1. In the absence of $AA_{2A}R$, the nor-

malized breakthrough time was not modified upon theophylline concentration and was equal to 1.3 thus revealing low non-specific interactions (Figure 1A). In addition, as expected for non-specific interactions, the amount of theophylline captured on empty nanodiscs column varied proportionally to its concentration (Figure 1B). In the presence of $AA_{2A}R$, the normalized breakthrough time increased as the theophylline concentration was decreased, as expected for specific interactions (Figure 1C). At the highest ligand concentrations, where non-specific interactions predominate, the normalized breakthrough time tends to 1.3, corresponding to the normalized breakthrough time value measured on empty nanodiscs and characteristic of non-specific interactions. The 1/q versus 1/[L] plot was linear and thus typical of one-site interaction (Figure 1D). Only a small deviation occurred for the highest concentrations (lowest 1/[L] range) due to non-specific interactions that contribute more significantly to the overall amount captured. Overall, non-specific binding is considered low as it accounts for less than 30 % of total binding for theophylline concentrations lower than 25 µM. Assuming that the total amount of ligand retained in the column corresponds to the sum of what is specifically interacting with a unique protein binding site, and of what is non-specifically interacting with the column surface and/or the nanodiscs particles, the calculated K_d value for theophylline was 32 ± 11 µM. This K_d value is consistent with values reported in the literature (25 µM[25]). The amount of active sites B_{act} was 7.2 ± 1.3 pmol (correlation coefficient 0.9997). Therefore, based on the known total protein content of the column (B_{tot} as equal to 11.3 pmol), the activity rate for $AA_{2A}R$ (B_{act}/B_{tot}) was 63 ± 11 %.

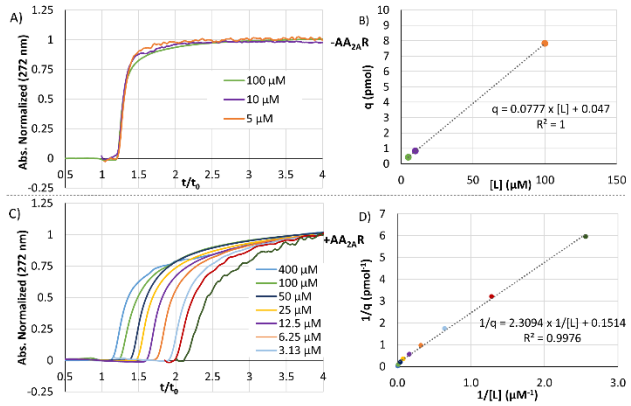

Figure 1. Frontal Affinity Chromatography analysis of the interaction between theophylline and immobilized nanodiscs columns (column dimensions: l=8.5 cm i.d.75 µm; applied pressure 12 MPa (0.14 $cm.s^{-1}$))

-$AA_{2A}R$ upper panels: empty nanodiscs. (A) Frontal affinity breakthrough curves (X-axis in reduced retention time t/t_0) on an empty-nanodiscs column. (B) Plot of captured quantities (q) versus ligand concentrations [L] and on an empty-nanodiscs column accounting for non-specific interactions.

+$AA_{2A}R$ lower panels: $AA_{2A}R$-nanodiscs. (C) Frontal affinity breakthrough curves (X-axis in reduced retention time t/t_0) on an $AA_{2A}R$-nanodiscs column. (D) Corresponding double reciprocal plot 1/q versus 1/[L] accounting for a one-site model.

For caffeine, similar breakthrough curves were observed in the presence of $AA_{2A}R$ (Figure S6). A K_d of 41 ± 15 µM was calculated, in good agreement with the literature (23.4 µM[25]). In addition, B_{act} was 11.6 ± 2.3 pmol (correlation coefficient 0.9999), indicating that the $AA_{2A}R$ activity rate was 104 ± 21 % with low non-specific interactions. Such high specific activities show that the grafting process is protein-friendly as it preserves the functionality of the nanodiscs-embedded $AA_{2A}R$.

Concerning the binding of adenosine in the presence of $AA_{2A}R$ (Figure 2), the normalized breakthrough time increased with decreased adenosine concentrations, as expected for specific interactions. However, a strong deviation from linearity was observed on the double reciprocal plot 1/q versus 1/[L], suggesting a multi-site interaction. As the adenosine has previously been reported to specifically bind streptavidin, a two-site model was used and turned out as the best-fit line. The calculated K_d values were 0.32 µM for the first site and 447 µM for the second (correlation coefficient 0.9998). These values are in good agreement with the reported values for the binding of the adenosine to $AA_{2A}R$ (0.7 µM[25]) or streptavidin (100-200 µM[43]). These results were further confirmed using FAC experiments carried out on control columns with either non-complexed streptavidin or immobilized empty nanodiscs (Figures S7 and S8). The amounts of active binding sites were also determined using the two-site model. The calculated values were 2.3 pmol for $AA_{2A}R$ resulting in an activity rate of approximatively 20 %, and 43 pmol for the streptavidin which is in good agreement with the expected amount of grafted streptavidin on the monolith[37].

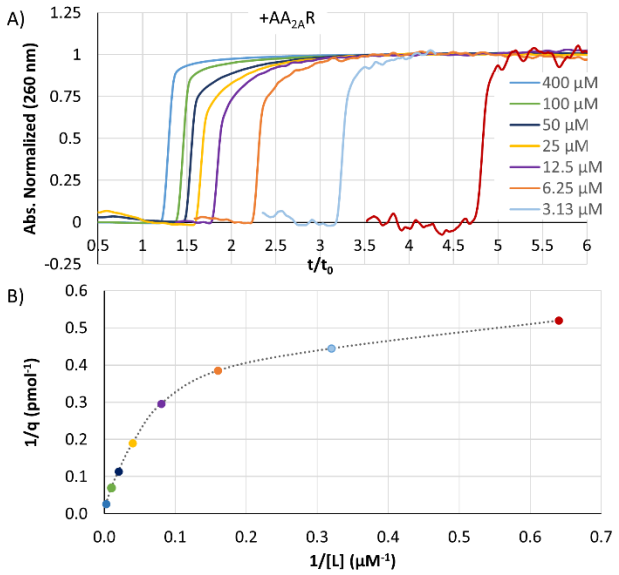

Figure 2. FAC analysis of the interaction between adenosine and immobilized $AA_{2A}R$ nanodiscs. (A) Frontal affinity breakthrough curves with adenosine at various concentrations X-axis in reduced retention time t/t_0; (B) double reciprocal plot 1/q versus 1/[L] accounting for a two-site model.

Competition experiments

In order to take the proof of concept a step further, ligand-binding experiments in a competition format were investigated. Competition experiments can be particularly valuable in the context of fragment screening to assess the binding site of fragments using a well-characterized competitor, or to serve as a control experiment for non-specific interactions. In the case of FAC experiments, the strategy involves a constant infusion

of the competitor into the column, first alone then with the monitored ligand. The chromatograms are analyzed by measuring the change in the breakthrough time of the monitored ligand in the absence and in the presence of the competitor: competition for the same binding site is expected to selectively reduce the breakthrough time.

Here, a competition experiment was achieved between theophylline and the high-affinity $AA_{2A}R$ antagonist ZM241385 (ZM). When 10 µM ZM was added in the mobile phase with theophylline, the breakthrough time shrank to a value close to the one obtained with theophylline alone on empty nanodiscs (Figure 3). This competition experiment confirmed that the interaction between theophylline and $AA_{2A}R$ nanodiscs, observed using the miniaturized FAC system, corresponds to a specific interaction in the orthosteric pocket of the protein.

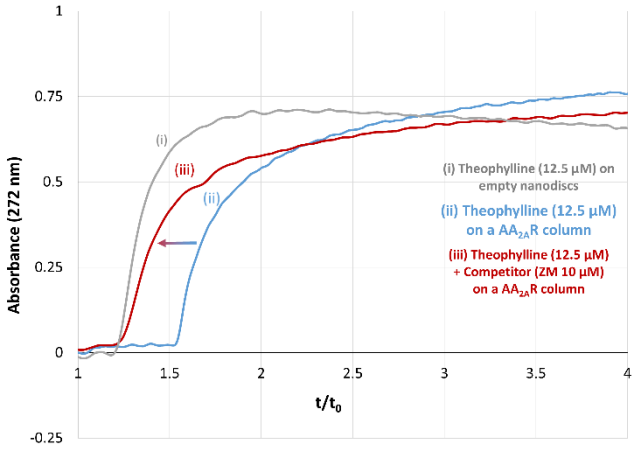

Figure 3. FAC analysis of the competition between theophylline and ZM241385 for the interaction with immobilized $AA_{2A}R$ nanodiscs. Frontal affinity breakthrough curves (X-axis in reduced retention time t/t_0) of a 12.5µM theophylline solution on (i) a control column with empty nanodiscs; (ii) on the $AA_{2A}R$-nanodiscs column without competitor; (iii) on the $AA_{2A}R$-nanodiscs column in presence of 10 µM ZM241385.

Identification of weak affinity ligands

Finally, the technique was tested for its capacity to identify weak affinity ligands such as fragments, and the possibility to discriminate weak affinity binders from non-binders, a particularly prominent issue with membrane proteins due to the presence of compounds used to maintain them in solution. The FAC strategy hitherto used to validate $AA_{2A}R$-ligand interactions, and shared by others[19,44], relies on the comparison of the normalized breakthrough times measured on columns grafted with protein over control columns (columns with empty-nanodiscs here). However, using control columns may lead to an overestimation of non-specific interactions due to the absence of the targeted protein, thus resulting in potential false negative signals as was previously suggested[19]. Since the normalized breakthrough time measured at high ligand concentrations in the presence of $AA_{2A}R$ is close to the one measured on the control column (Figure 1) an alternative approach relies on the comparison between the normalized breakthrough times for two extreme fragment concentrations on a single column containing the immobilized protein. Nonetheless, since the measures are realized on the same column, this strategy further avoids uncertainties associated with column variability due to the grafting efficacy. In order to determine what those extreme concentrations should be, normalized breakthrough time differences were simulated for several K_d values and various fragment concentrations. For the lowest affinities, 10 and 1000 µM showed the most significant discrepancy (Figure S9). With this set-up, and a minimal difference in normalized breakthrough time fixed at 10 %, K_d values as high as 250 µM are detectable.

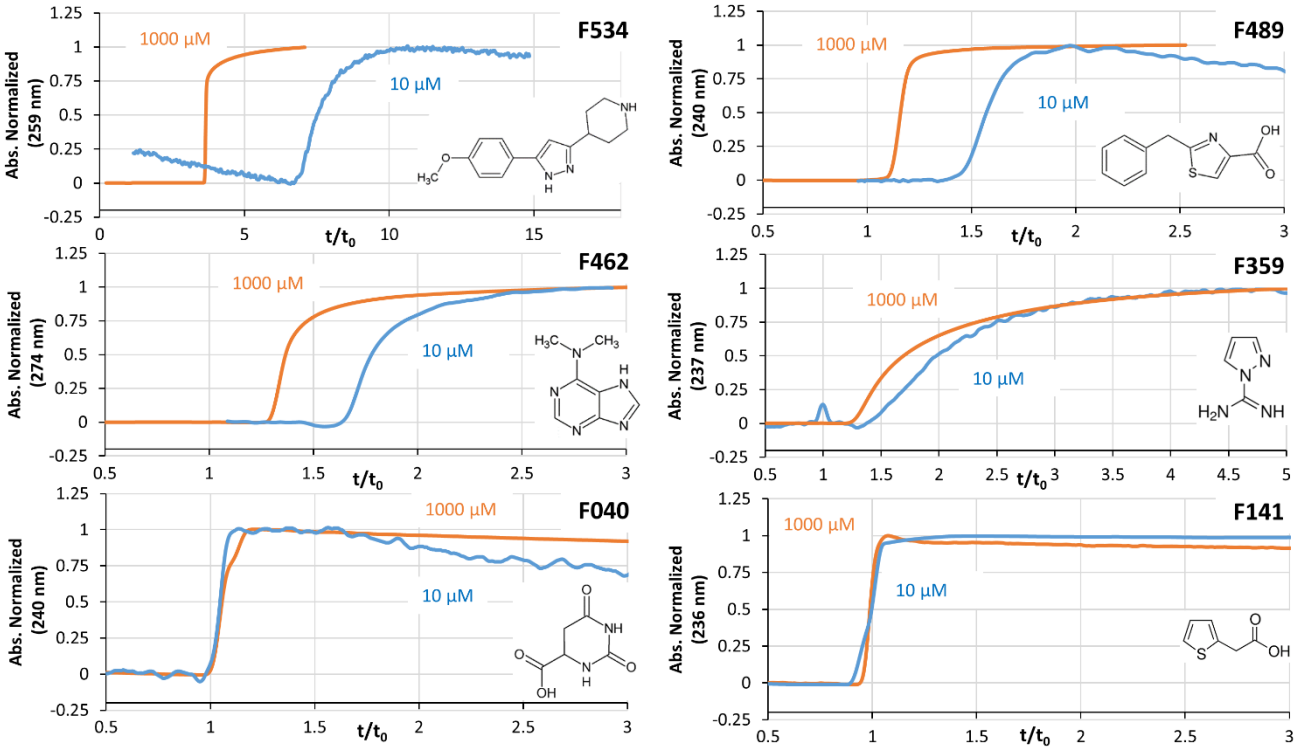

Figure 4. FAC analysis of fragments interaction with immobilized $AA_{2A}R$ nanodiscs. Frontal affinity breakthrough curves obtained on an $AA_{2A}R$-nanodiscs column for several fragments prepared in a 67 mM phosphate pH 7.4 buffer.

This approach was applied to six fragments selected from a published NMR screening carried out on $AA_{2A}R$ in detergent micelles[13] (see Figure S2 for compounds structures). Four of them were shown to bind $AA_{2A}R$ using STD-NMR experiments, while two were shown not to. As illustrated in Figure 4, significant differences between normalized breakthrough times measured at low and high concentrations were observed for fragments F534, F489, F462 and F359, whereas fragments F040 and F141 displayed identical normalized breakthrough times regardless of the concentration. Consequently, F534, F489, F462 and F359 were identified as ligands of $AA_{2A}R$ while F040 and F141 were identified as non-ligands. These results are in perfect agreement with the previously reported STD-NMR data[13]. Because the higher the normalized breakthrough time discrepancy, the higher the affinity for the target, these FAC experiments also allow a ranking of the ligands according to their increased affinities, starting from F359 than F462 and F489 and F534.

CONCLUSION

Here we have shown for the first time that lipid-nanodiscs systems and ultra-miniaturized affinity chromatography can be combined to identify specific small molecule ligands that bind to an integral membrane protein. The approach was exemplified using the $AA_{2A}R$ GPCR. Specific and unspecific ligand/receptor interactions were distinguished using empty nanodiscs as a negative control. Competition experiments can be performed to identify the binding pocket of uncharacterized ligands using a reference compound. Weak affinity ligands with K_d smaller than 250 µM should be detected. At last, the applicability of this method was demonstrated with 6 fragments recently identified as ligands or non-ligands of $AA_{2A}R$. Here, experiments were carried out at two extreme concentrations on a unique affinity column.

Besides being a suitable membrane-mimicking environment for $AA_{2A}R$, the use of nanodiscs also offers multiple advantages with regards to the grafting procedure. $AA_{2A}R$ is not itself tethered to the stationary phase but through the biotinylated MSP that enables a homogenous oriented immobilization, and the presence of the spacer arm ensures a full accessibility of the binding pocket to small molecules. $AA_{2A}R$ remains full native, as evidenced by the high specific activities obtained. The strong and rapid biotin-streptavidin interaction associated with the UV-monitoring of the grafting step permits the use of the exact amount of grafted protein and a very rapid grafting step. The reduction of both the grafting duration and protein consumption represent two tremendous assets for proteins that are difficult to produce and that present a limited stability. A column contains only 0.6 µg of $AA_{2A}R$ on average (14 pmol). Streptavidin columns can be prepared in advance, stored for several months (4°C) before being grafted with the target of interest.

The method reported here is applicable to any membrane protein reconstituted in biotinylated nanodiscs and offers a real potential for FBDD on membrane proteins. Its coupling with mass spectrometry via a nanospray interface, should allow a rapid screening of a library (for a 30 min total analysis time, and considering mixtures of 10-20 compounds, 500 to 1000 compounds should be screened in one day, with a minimal protein consumption and with reduced stability issues).

ASSOCIATED CONTENT

Supporting Information

The Supporting Information is available free of charge on the ACS Publications website.

Supplementary methods, results and figures (PDF)

AUTHOR INFORMATION

Corresponding Author

* Tel.: +33437423552
E-mail address: claire.demesmay@univ-lyon1.fr

ACKNOWLEDGMENT

The authors are grateful to the Imaging Center of the IGBMC (Illkirch) for the electron microscopy data.

REFERENCES

(1) Hauser, A. S.; Attwood, M. M.; Rask-Andersen, M.; Schiöth, H. B.; Gloriam, D. E. Trends in GPCR Drug Discovery: New Agents, Targets and Indications. *Nature Reviews Drug Discovery* **2017**, *16* (12), 829–842. https://doi.org/10.1038/nrd.2017.178.

(2) Shimada, I.; Ueda, T.; Kofuku, Y.; Eddy, M. T.; Wüthrich, K. GPCR Drug Discovery: Integrating Solution NMR Data with Crystal and Cryo-EM Structures. *Nat Rev Drug Discov* **2018**. https://doi.org/10.1038/nrd.2018.180.

(3) Ghosh, E.; Kumari, P.; Jaiman, D.; Shukla, A. K. Methodological Advances: The Unsung Heroes of the GPCR Structural Revolution. *Nature Reviews Molecular Cell Biology* **2015**, *16* (2), 69–81. https://doi.org/10.1038/nrm3933.

(4) Cooke, R. M.; Brown, A. J. H.; Marshall, F. H.; Mason, J. S. Structures of G Protein-Coupled Receptors Reveal New Opportunities for Drug Discovery. *Drug Discovery Today* **2015**, *20* (11), 1355–1364. https://doi.org/10.1016/j.drudis.2015.08.003.

(5) Andrews, S. P.; Brown, G. A.; Christopher, J. A. Structure-Based and Fragment-Based GPCR Drug Discovery. *ChemMedChem* **2014**, *9* (2), 256–275. https://doi.org/10.1002/cmdc.201300382.

(6) Jhoti, H.; Williams, G.; Rees, D. C.; Murray, C. W. The "rule of Three" for Fragment-Based Drug Discovery: Where Are We Now? *Nature Reviews Drug Discovery* **2013**, *12* (8), 644–644. https://doi.org/10.1038/nrd3926-c1.

(7) Erlanson, D. A.; Fesik, S. W.; Hubbard, R. E.; Jahnke, W.; Jhoti, H. Twenty Years on: The Impact of Fragments on Drug Discovery. *Nature Reviews Drug Discovery* **2016**, *15* (9), 605–619. https://doi.org/10.1038/nrd.2016.109.

(8) Meiby, E.; Simmonite, H.; le Strat, L.; Davis, B.; Matassova, N.; Moore, J. D.; Mrosek, M.; Murray, J.; Hubbard, R. E.; Ohlson, S. Fragment Screening by Weak Affinity Chromatography: Comparison with Established Techniques for Screening against HSP90. *Anal. Chem.* **2013**, *85* (14), 6756–6766. https://doi.org/10.1021/ac400715t.

(9) Duong-Thi, M.-D.; Meiby, E.; Bergström, M.; Fex, T.; Isaksson, R.; Ohlson, S. Weak Affinity Chromatography as a New Approach for Fragment Screening in Drug Discovery. *Analytical Biochemistry* **2011**, *414* (1), 138–146. https://doi.org/10.1016/j.ab.2011.02.022.

(10) Duong-Thi, M.-D.; Bergström, M.; Fex, T.; Isaksson, R.; Ohlson, S. High-Throughput Fragment Screening by Affinity LC-MS. *J Biomol Screen* **2013**, *18* (2), 160–171. https://doi.org/10.1177/1087057112459271.

(11) Tsopelas, F.; Tsantili-Kakoulidou, A. Advances with Weak Affinity Chromatography for Fragment Screening. *Expert Opinion on Drug Discovery* **2019**, *0* (0), 1–11. https://doi.org/10.1080/17460441.2019.1648425.

(12) Murray, C. W.; Verdonk, M. L.; Rees, D. C. Experiences in Fragment-Based Drug Discovery. *Trends in Pharmacological Sciences* **2012**, *33* (5), 224–232. https://doi.org/10.1016/j.tips.2012.02.006.

(13) Igonet, S.; Raingeval, C.; Cecon, E.; Pučić-Baković, M.; Lauc, G.; Cala, O.; Baranowski, M.; Perez, J.; Jockers, R.; Krimm, I.; et al. Enabling STD-NMR Fragment Screening Using Stabilized Native GPCR: A Case Study of Adenosine Receptor. *Scientific Reports* **2018**, *8* (1). https://doi.org/10.1038/s41598-018-26113-0.

(14) Chen, D.; Errey, J. C.; Heitman, L. H.; Marshall, F. H.; IJzerman, A. P.; Siegal, G. Fragment Screening of GPCRs Using Biophysical Methods: Identification of Ligands of the Adenosine A_{2A} Receptor with Novel Biological Activity. *ACS Chemical Biology* **2012**, *7* (12), 2064–2073. https://doi.org/10.1021/cb300436c.

(15) Congreve, M.; Rich, R. L.; Myszka, D. G.; Figaroa, F.; Siegal, G.; Marshall, F. H. Fragment Screening of Stabilized G-Protein-Coupled Receptors Using Biophysical Methods. In *Methods in Enzymology*; Elsevier, 2011; Vol. 493, pp 115–136. https://doi.org/10.1016/B978-0-12-381274-2.00005-4.

(16) Aristotelous, T.; Ahn, S.; Shukla, A. K.; Gawron, S.; Sassano, M. F.; Kahsai, A. W.; Wingler, L. M.; Zhu, X.; Tripathi-Shukla, P.; Huang, X.-P.; et al. Discovery of B2 Adrenergic Receptor Ligands Using Biosensor Fragment Screening of Tagged Wild-Type Receptor. *ACS Medicinal Chemistry Letters* **2013**, *4* (10), 1005–1010. https://doi.org/10.1021/ml400312j.

(17) Christopher, J. A.; Brown, J.; Doré, A. S.; Errey, J. C.; Koglin, M.; Marshall, F. H.; Myszka, D. G.; Rich, R. L.; Tate, C. G.; Tehan, B.; et al. Biophysical Fragment Screening of the β_1-Adrenergic Receptor: Identification of High Affinity Arylpiperazine Leads Using Structure-Based Drug Design. *Journal of Medicinal Chemistry* **2013**, *56* (9), 3446–3455. https://doi.org/10.1021/jm400140q.

(18) Navratilova, I.; Besnard, J.; Hopkins, A. L. Screening for GPCR Ligands Using Surface Plasmon Resonance. *ACS Medicinal Chemistry Letters* **2011**, *2* (7), 549–554. https://doi.org/10.1021/ml2000017.

(19) Duong-Thi, M.-D.; Bergström, M.; Edwards, K.; Eriksson, J.; Ohlson, S.; To Yiu Ying, J.; Torres, J.; Agmo Hernández, V. Lipodisks Integrated with Weak Affinity Chromatography Enable Fragment Screening of Integral Membrane Proteins. *The Analyst* **2016**, *141* (3), 981–988. https://doi.org/10.1039/C5AN02105G.

(20) Fredriksson, K.; Lottmann, P.; Hinz, S.; Onila, I.; Shymanets, A.; Harteneck, C.; Müller, C. E.; Griesinger, C.; Exner, T. E. Nanodiscs for INPHARMA NMR Characterization of GPCRs: Ligand Binding to the Human A2A Adenosine Receptor. *Angewandte Chemie International Edition* **2017**, *56* (21), 5750–5754. https://doi.org/10.1002/anie.201612547.

(21) Bocquet, N.; Kohler, J.; Hug, M. N.; Kusznir, E. A.; Rufer, A. C.; Dawson, R. J.; Hennig, M.; Ruf, A.; Huber, W.; Huber, S. Real-Time Monitoring of Binding Events on a Thermostabilized Human A2A Receptor Embedded in a Lipid Bilayer by Surface Plasmon Resonance. *Biochimica et Biophysica Acta (BBA) - Biomembranes* **2015**, *1848* (5), 1224–1233. https://doi.org/10.1016/j.bbamem.2015.02.014.

(22) Silvia, L.-H.; A, Y. A.; Klaus, G.; Inna, G. Surface Plasmon Resonance Applied to G Protein-Coupled Receptors. *Biomedical Spectroscopy and Imaging* **2013**, No. 3, 155–181. https://doi.org/10.3233/BSI-130045.

(23) Bayburt, T. H.; Sligar, S. G. Membrane Protein Assembly into Nanodiscs. *FEBS Lett.* **2010**, *584* (9), 1721–1727. https://doi.org/10.1016/j.febslet.2009.10.024.

(24) Serebryany, E.; Zhu, G. A.; Yan, E. C. Y. Artificial Membrane-like Environments for in Vitro Studies of Purified G-

Protein Coupled Receptors. *Biochim. Biophys. Acta* **2012**, *1818* (2), 225–233. https://doi.org/10.1016/j.bbamem.2011.07.047.

(25) de Lera Ruiz, M.; Lim, Y.-H.; Zheng, J. Adenosine A 2A Receptor as a Drug Discovery Target. *Journal of Medicinal Chemistry* **2014**, *57* (9), 3623–3650. https://doi.org/10.1021/jm4011669.

(26) Müller, C. E.; Jacobson, K. A. Recent Developments in Adenosine Receptor Ligands and Their Potential as Novel Drugs. *Biochimica et Biophysica Acta (BBA) - Biomembranes* **2011**, *1808* (5), 1290–1308. https://doi.org/10.1016/j.bbamem.2010.12.017.

(27) Carpenter, B.; Lebon, G. Human Adenosine A2A Receptor: Molecular Mechanism of Ligand Binding and Activation. *Frontiers in Pharmacology* **2017**, *8*. https://doi.org/10.3389/fphar.2017.00898.

(28) Pinna, A. Adenosine A2A Receptor Antagonists in Parkinson's Disease: Progress in Clinical Trials from the Newly Approved Istradefylline to Drugs in Early Development and Those Already Discontinued. *CNS Drugs* **2014**, *28* (5), 455–474. https://doi.org/10.1007/s40263-014-0161-7.

(29) Franco, R.; Navarro, G. Adenosine A2A Receptor Antagonists in Neurodegenerative Diseases: Huge Potential and Huge Challenges. *Frontiers in Psychiatry* **2018**, *9*. https://doi.org/10.3389/fpsyt.2018.00068.

(30) Sek, K.; Mølck, C.; Stewart, G.; Kats, L.; Darcy, P.; Beavis, P. Targeting Adenosine Receptor Signaling in Cancer Immunotherapy. *International Journal of Molecular Sciences* **2018**, *19* (12), 3837. https://doi.org/10.3390/ijms19123837.

(31) Chen, J.-F.; Eltzschig, H. K.; Fredholm, B. B. Adenosine Receptors as Drug Targets — What Are the Challenges? *Nature Reviews Drug Discovery* **2013**, *12* (4), 265–286. https://doi.org/10.1038/nrd3955.

(32) Hartmann, L.; Kugler, V.; Wagner, R. Expression of Eukaryotic Membrane Proteins in Pichia Pastoris. *Methods Mol. Biol.* **2016**, *1432*, 143–162. https://doi.org/10.1007/978-1-4939-3637-3_10.

(33) Denisov, I. G.; Grinkova, Y. V.; Lazarides, A. A.; Sligar, S. G. Directed Self-Assembly of Monodisperse Phospholipid Bilayer Nanodiscs with Controlled Size. *J. Am. Chem. Soc.* **2004**, *126* (11), 3477–3487. https://doi.org/10.1021/ja0393574.

(34) Hansen, R. W.; Wang, X.; Golab, A.; Bornert, O.; Oswald, C.; Wagner, R.; Martinez, K. L. Functional Stability of the Human Kappa Opioid Receptor Reconstituted in Nanodiscs Revealed by a Time-Resolved Scintillation Proximity Assay. *PLoS ONE* **2016**, *11* (4), e0150658. https://doi.org/10.1371/journal.pone.0150658.

(35) Bruchet, A.; Dugas, V.; Mariet, C.; Goutelard, F.; Randon, J. Improved Chromatographic Performances of Glycidyl Methacrylate Anion-Exchange Monolith for Fast Nano-Ion Exchange Chromatography. *Journal of Separation Science* **2011**, *34* (16-17 Special Issue), 2079–2087. https://doi.org/10.1002/jssc.201100180.

(36) Faye, C.; Chamieh, J.; Moreau, T.; Garnier, F.; Faure, K.; Dugas, V.; Demesmay, C.; Vandenabeele-Trambouze, O. In Situ Characterization of Antibody Grafting on Porous Monolithic Supports. *Analytical Biochemistry* **2012**, *420* (2), 147–154. https://doi.org/10.1016/j.ab.2011.09.016.

(37) Lecas, L.; Randon, J.; Berthod, A.; Dugas, V.; Demesmay, C. Monolith Weak Affinity Chromatography for Mg-Protein-Ligand Interaction Study. *Journal of Pharmaceutical and Biomedical Analysis* **2019**, *166*, 164–173. https://doi.org/10.1016/j.jpba.2019.01.012.

(38) André, N.; Cherouati, N.; Prual, C.; Steffan, T.; Zeder-Lutz, G.; Magnin, T.; Pattus, F.; Michel, H.; Wagner, R.; Reinhart, C. Enhancing Functional Production of G Protein-Coupled Receptors in Pichia Pastoris to Levels Required for Structural Studies via a Single Expression Screen. *Protein Sci* **2006**, *15* (5), 1115–1126. https://doi.org/10.1110/ps.062098206.

(39) Fredholm, B. B.; IJzerman, A. P.; Jacobson, K. A.; Klotz, K. N.; Linden, J. International Union of Pharmacology. XXV. Nomenclature and Classification of Adenosine Receptors. *Pharmacol. Rev.* **2001**, *53* (4), 527–552.

(40) Duong-Thi, M.-D.; Bergström, M.; Fex, T.; Svensson, S.; Ohlson, S.; Isaksson, R. Weak Affinity Chromatography for Evaluation of Stereoisomers in Early Drug Discovery. *Journal of Biomolecular Screening* **2013**, *18* (6), 748–755. https://doi.org/10.1177/1087057113480391.

(41) Ohlson, S.; Duong-Thi, M.-D. Fragment Screening for Drug Leads by Weak Affinity Chromatography (WAC-MS). *Methods* **2018**, *146*, 26–38. https://doi.org/10.1016/j.ymeth.2018.01.011.

(42) Matsuda, R.; Li, Z.; Zheng, X.; Hage, D. S. Analysis of Multi-Site Drug–Protein Interactions by High-Performance Affinity Chromatography: Binding by Glimepiride to Normal or Glycated Human Serum Albumin. *Journal of Chromatography A* **2015**, *1408*, 133–144. https://doi.org/10.1016/j.chroma.2015.07.012.

(43) Bing, T.; Chang, T.; Qi, C.; Zhang, N.; Liu, X.; Shangguan, D. Specific Interactions between Adenosine and Streptavidin/Avidin. *Bioorganic & Medicinal Chemistry Letters* **2012**, *22* (23), 7052–7055. https://doi.org/10.1016/j.bmcl.2012.09.088.

(44) Conrad, M. L.; Moser, A. C.; Hage, D. S. Evaluation of Indole-Based Probes for High-Throughput Screening of Drug Binding to Human Serum Albumin: Analysis by High-Performance Affinity Chromatography. *Journal of Separation Science* **2009**, *32* (8), 1145–1155. https://doi.org/10.1002/jssc.200800567.